Urban Climate 64 (2025) 102681

Contents lists available at ScienceDirect

Urban Climate

journal homepage: www.elsevier.com/locate/uclim

Potential impact of climate change on heatwaves at the urban scale: An evaluation in Valencia, Spain

Ana Fernandez-Garza [a,*], Eric Gielen [b], Manuel Pulido-Velazquez [a], Dariana Avila-Velasquez [a], Adria Rubio-Martin [a], Hector Macian-Sorribes [a]

[a] IIAMA, Universitat Politècnica de València, Valencia, Spain
[b] Dpto de Urbanismo, Universitat Politècnica de València, Valencia, Spain

ARTICLE INFO

Keywords:
Heatwaves
Climate projections
Heat index
Temperature
Humidity

ABSTRACT

Global temperatures have risen rapidly over the past six decades, with the Mediterranean region recognized as a climate hotspot due to its accelerated warming and declining precipitation. In this context, heatwaves have become more frequent, longer, and more intense, causing growing risks to human health, ecosystems, and urban resilience.

This study aims to quantify the historical (1979–2014) and projected (up to 2100) evolution of heatwaves in Valencia, Spain. Daily maximum temperatures (°C) and relative humidity (%) from five CMIP6 global climate models under three emission scenarios were used, complemented with observational records. The heat index is used to better assess the impact of heat on human health. Temporal trend analyses and spatial interpolation are applied to assess changes in frequency, duration and intensity. Results show that during 1979–2014, the heatwave frequency increased by approximately two events per decade, while their mean duration rose from under 10 to nearly 25 days. Under future scenarios, intensification continues: by mid-century frequency may increase by up, 3.6 additional events per decade, and toward the end of the century there seems to be shift toward a quasi-permanent heat season, as episodes merge into fewer but longer events. Rising humidity further amplifies thermal stress, enhancing the human health impact.

Despite uncertainties inherent in climate projections, these findings highlight the need to revisit heatwave definitions refine thermal risk thresholds, and adopt robust adaptation strategies for Mediterranean cities.

1. Introduction

Heatwaves, fueled by rising greenhouse gas concentrations, are becoming more frequent, intense, and prolonged, posing escalating risks to human health, economies, and ecosystems worldwide (Hirsch et al., 2021; Sun et al., 2023). These extreme temperature events have surged in prominence over recent decades, with historic examples like the 2003 European heatwave, the 2010 Russian crisis, the 2018–2019 European drought sequence, the 2021 Canadian anomaly, and the 2023 Global heat event; leaving devastating trails of mortality, wildfires, and economic disruption (Hari et al., 2020; Hirsch et al., 2021; Min and Merwin Monteiro, 2025; Sun et al., 2023). Research shows with high confidence that human-driven climate change has amplified these events, making many unlikely without

* Corresponding author.
E-mail addresses: agferga1@alumni.upv.es (A. Fernandez-Garza), egielen@urb.upv.es (E. Gielen), mapuve@hma.upv.es (M. Pulido-Velazquez), diavivel@upvnet.upv.es (D. Avila-Velasquez), adrumar@upv.es (A. Rubio-Martin), hecmasor@upv.es (H. Macian-Sorribes).

https://doi.org/10.1016/j.uclim.2025.102681
Received 7 July 2025; Received in revised form 16 October 2025; Accepted 29 October 2025
Available online 8 November 2025

our influence (Klingelhöfer et al., 2023; Perkins-Kirkpatrick and Lewis, 2020; Van Oldenborgh et al., 2022). Even if global warming were stabilized at 1.5 °C, target increasingly unlikely under current trajectories, studies warn that heatwave trends will persist, challenging societies to adapt (Yin et al., 2022).

Globally, heatwave patterns reveal stark regional variations. From 1950 to 2017, most areas saw intensity increases of 2–6 °C per decade and durations extended by one day per decade (Perkins-Kirkpatrick and Lewis, 2020). In the Middle East, Africa, and South America, intensity spikes reached 10 °C per decade, while India anticipates 0.5 more events and 4–7 extra days per decade through 2064 (Rohini et al., 2019). Australia, between 1911 and 2019, recorded 0.4–0.6 additional events and 2.5 °C hotter heatwaves per decade (Jyoteeshkumar Reddy et al., 2021). In Central Europe, projections suggest temperature rises up to 5 °C by century's end, with heatwaves lasting 10–60 days longer depending on emissions (Lhotka et al., 2018; Ouzeau et al., 2016). These trends, driven by advanced modeling, highlight a warming world where extremes are the new norm.

In this global context, the Mediterranean emerges as a climate hotspot, where warming outpaces other regions, and unique geographic challenges amplify heatwave impacts (Cos et al., 2022). Positioned between North Africa's arid heat and Europe's temperate humidity, the region experiences summer temperature increases 1.6 times the global average (Cos et al., 2022). Recent projections based on the latest generation of climate models indicate alarming rises up to 8.49 °C in summer temperatures, alongside declining precipitation, intensifying heatwave intensity across the Mediterranean region (Cos et al., 2022; Intergovernmental Panel on Climate Change (IPCC), 2023).

Within this hotspot, the Iberian Peninsula shows a marked uptick in heatwave frequency and extent (Díaz-Poso et al., 2023). This region, located at the western edge of the Mediterranean basin, combines Mediterranean and Atlantic influences, with further modulate extreme temperature events. At the local scale, Valencia, a coastal Mediterranean city, exemplifies these trends. Its 2023 summer, one of the hottest on record, exceeded the 1991–2020 average by 2 °C, peaking at 46.8 °C (Agencia Estatal de Meteorología, 2023). Such extremes underscore the direct local toll of a warming planet.

In the Mediterranean region, the Coupled Model Intercomparison Project Phase 6 (CMIP6) serve as a crucial foundation for contemporary climate research, improving upon earlier model generations by using updated socio-economic pathways and enhanced process representation. These improvements provide a more reliable basis for regional analyses, even as ongoing downscaling initiatives such as ISMIP continue to refine spatial detail (Eyring et al., 2016a). CMIP6 models have introduced several improvements in the representation of radiation, clouds, and aerosols compared to CMIP5. These include updated cloud microphysics schemes, more accurate aerosol, radiation interactions, and higher spatial resolution, which together allow for a more realistic simulation of cloud cover, precipitation processes, and radiative forcing. As a result, CMIP6 provides more detailed and reliable projections of temperature and precipitation extremes, particularly during heatwaves (Eyring et al., 2016b). Nevertheless, differences in the magnitude of the projections persist, particularly during the summer, with a temperature increase range of 1.83–8.49 °C in CMIP6 versus 1.22–6.63 °C in CMIP5. To capture regional variability more effectively, this study recommends subdividing the Mediterranean into smaller subregions, considering local climatic particularities (Cos et al., 2022). Despite these advances, critical gaps remain in densely populated and vulnerable areas, as regional climate models often fail to account for crucial variables influencing human exposure and vulnerability, which limits the accuracy of risk assessment (Cos et al., 2022; Ouzeau et al., 2016).

Heatwaves are commonly assessed using multiple indicators, including intensity, frequency, and duration, typically defined by temperature thresholds exceeding the 90th percentile for a minimum of two consecutive days (Robinson, 2000). However, these metrics mainly focus on air temperature and tend to overlook other critical factors contributing to human stress. Among these, relative humidity plays a central role, as it reduces the body's ability to dissipate heat, complicating thermoregulation. Therefore, it is essential to incorporate complementary indices, such as the heat index, that better reflect human thermal perception and health risks (Cos et al., 2022; Monteiro et al., 2013; Ouzeau et al., 2016).

The heat index is one such indicator, designed to estimate perceived temperature by integrating air temperature and relative humidity. In the Mediterranean city of Porto, studies have validated its usefulness in anticipating the negative health impacts of heatwaves, making it a reliable predictor of heat-related mortality (Monteiro et al., 2013). However, despite its potential, the heat index remains underutilized in regional climate projections. Without integrating such complementary metrics, risk assessments of heatwaves and their interactions with droughts and wildfires may fall short, particularly for the most vulnerable populations (Zuo et al., 2015).

Vulnerability is commonly defined as the degree to which a population is susceptible to and unable to cope with adverse effects, determined by the interaction of exposure, sensitivity, and adaptive capacity. In other words, it reflects the stresses to which individuals are exposed, their inherent sensitivity, and their capacity to adapt (Adger, 2006). From this perspective, vulnerability to extreme heat is inherently heterogeneous, as it stems from both social and physiological dimensions. Socioeconomic conditions and characteristics of the living environment can amplify or mitigate heat impacts (Díaz et al., 2019). During heatwaves, humidity plays a critical physiological role in thermoregulation by limiting heat dissipation through sweat evaporation, thereby intensifying heat stress and related health risks (Awasthi et al., 2022; Porja and Dhimitri, 2019; Royé et al., 2020). Furthermore, age-related differences condition susceptibility: older adults and children often present reduced thermoregulatory capacity, greater dependence, or heightened exposure (Falchetta et al., 2024; Wei and Sobrino, 2024; Zacharias et al., 2015).

The purpose of this study is to analyze the historical and future evolution of heatwaves in the Mediterranean, with a focus on the city of Valencia, Spain, from 1979 to 2100, using five CMIP6 climate models. Heatwave's frequency, intensity, and duration are evaluated under different emission scenarios (SSP126, SSP370, and SSP585). Heatwaves are identified using established thresholds, such as maximum temperatures exceeding the 90th percentile for three or more consecutive days, while incorporating variables like duration, intensity, and the heat index, which accounts for both temperature and relative humidity, to capture human-perceived heat stress. The new metrics allow for precise evaluation of health risks linked to changing climate patterns. Changes in the number of heatwave events, their duration in the short, medium and long term and the expansion of high-temperature periods in the future will also be analyzed. By spanning past trends and future possibilities through 2100, this analysis seeks to quantify risks.

This study stands out by integrating **relative humidity**, into **long-term heatwave assessments** from 1979 to 2100 and presents new evidence of how extreme heat may evolve into permanent summer conditions, challenging existing definitions of heatwaves and risk frameworks.

The paper is structured as follows: Materials and Methods details our data sources, CMIP6 models, and analytical approach, including heatwave definitions and heat index calculations. Results present historical trends and future projections for Valencia, supported by visual diagrams and heat maps. Discussion compares findings to global patterns, explores implications, and addresses model limitations. Finally, Conclusions synthesize key insights and propose strategies to mitigate heatwave impacts, emphasizing local relevance.

2. Materials and methods

2.1. Study area

The study focuses on the city of Valencia, Spain, within the Valencian Region (Fig. 1, A). The study area is bounded by the V-21, CV-35, and V-30 highways and the Mediterranean coastline, extending from the Turia River outlet to La Patacona beach (Fig. 1, B). It covers 52.1 km^2 across seven municipalities, including Valencia, Alboraya, Burjassot, Xirivella, Quart de Poblet, Mislata, and Paterna. Despite representing only 2 % of the Metropolitan Area of Valencia, it houses 65 % of its population, exceeding one million inhabitants.

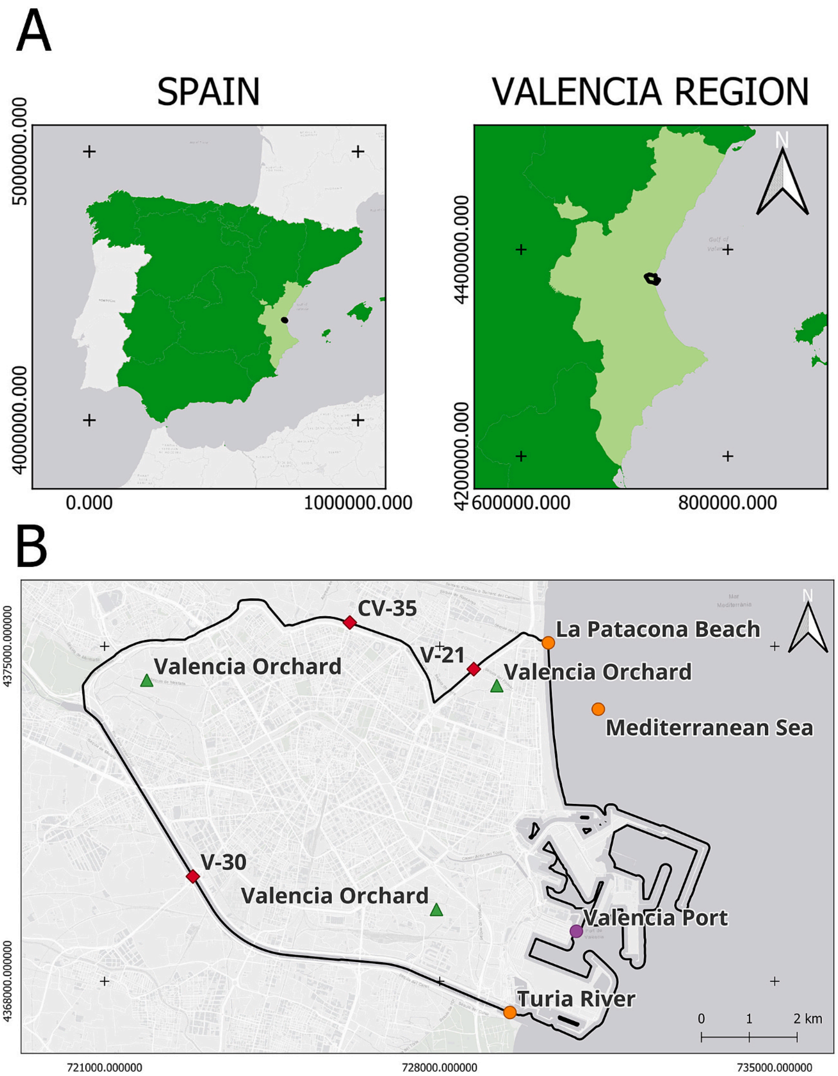

Fig. 1. Location of the study area: (a) Spain with the Valencia Region highlighted, (b) Detailed map of the urban and peri urban study area.

Economically, the area is dominated by the service sector, which employs 84 % of the workforce, with notable activities in trade, business services, and tourism. The industrial sector, comprising 11 % of employment, includes small and medium-sized enterprises in paper, furniture, and metal production. Agriculture remains relevant due to the presence of the historic Valencia Orchard (Ajuntament de València, 2025).

The region experiences a Mediterranean climate, with hot, humid summers and mild winters. The average annual temperature is 18 °C, with August being the warmest month (30 °C) and January the coldest (6 °C). High humidity is persistent, peaking between June and October. Winds shift seasonally, blowing from the west in winter and the east in summer. Rainfall is concentrated between September and May, with October as the wettest month, while summers are mostly dry and clear (Cedar Lake Ventures, 2025).

Within this context, two population groups are particularly vulnerable to heatwaves. Children up to 12 years old are at higher risk due to their physiology and limited ability to regulate body temperature, with boys generally outnumbering girls, especially in municipalities such as Alboraya, Burjassot, and Quart de Poblet. This group represents around 13 % of the total population. Older adults, aged 60 and above, are also highly vulnerable due to preexisting health conditions and reduced capacity to adapt to heat. In contrast to children, women outnumber men in this age group, a pattern that becomes more pronounced after age 75; for example, in Burjassot, women nearly double the number of men. Overall, older men account for 9.63 % of the population (98,026), and older women for 13.53 % (137,781), totaling 23.15 % (235,807) (Agencia Estatal de Meteorología, 2023; Instituto Nacional de Estadística, 2024).

3. Methods

This study analyzes heatwave characteristics in the Valencian Region using a climate database that compiles daily records of maximum temperature and relative humidity from 1979 to 2100. Climate projections are derived from multiple global climate models, which provide data under different Shared Socioeconomic Pathways (SSPs). The historical period (1979–2014) serves as a baseline for comparison with future projections. The study area is defined using a high-resolution spatial grid, allowing detailed climate analysis (Lange, 2019b; O'Neill et al., 2016; Peano et al., 2022).

Heatwaves are identified based on established meteorological criteria, defining them as periods of at least three consecutive days where maximum temperatures exceed a critical threshold. This threshold corresponds to the 90th percentile of historical daily maximum temperatures and is determined for each month. Heatwave events are characterized by key metrics, including duration, frequency, and intensity. Additionally, the study assesses human exposure to extreme heat by calculating the Heat Index (HI), an empirical measure that integrates temperature and relative humidity. For each detected heatwave event, the following parameters are recorded: start and end dates, duration, maximum temperature, sum of thermal anomalies, and sum of heat index anomalies.

To evaluate long-term trends in heatwave characteristics, linear regression models are applied across different time periods, estimating annual rates of change. This analysis is complemented by bubble charts and heat maps, that display changes in frequency, duration, intensity and temporal patterns. This methodological approach provides a comprehensive assessment of heatwaves and their projected impact under different climate scenarios.

To provide a clearer understanding of the analytical process, the methodology is summarized in the following Fig. 2 and is divided into two main components: A) Heatwave characterization and B) Trend analysis. Part A focuses on the detection and quantification of heatwave events using key parameters. Part B addresses the evaluation of trends by applying statistical analyses and visual tools to explore the evolution of extreme heat events over time. The following sections presents a detailed explanation of each part of the methodology.

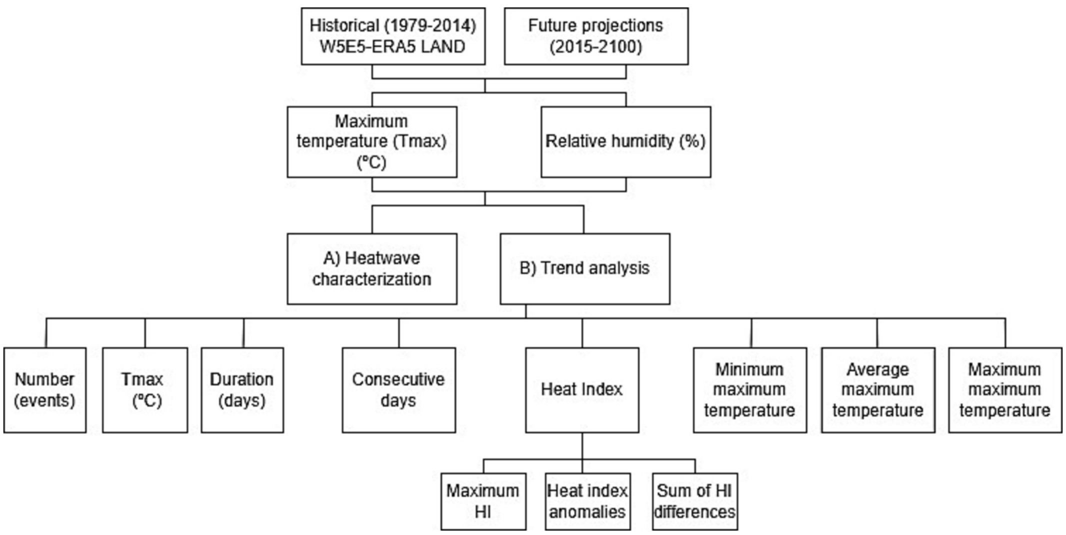

Fig. 2. Methodology flowchart summarizing the steps for heatwave characterization and trend analysis based on temperature and relative humidity data.

3.1.1. Heatwave characterization

The analysis is based on a database that compiles daily information on maximum temperature and relative humidity from 1979 to 2100. This data includes one observed database, the W5E5 database bias-corrected to the ERA5-Land scale for the historical period 1979–2014 (Lange, 2019b; O'Neill et al., 2016; Peano et al., 2022), and projections from five climate models from CMIP6. The study area located in the Valencian Region, where the data were organized according to the W5E5-ERA5-Land grid, with an approximate spatial resolution of 9 km, covering four grid points: (39.5; −0.4); (39.5; −0.3); (39.4; −0.4) and (39.4; −0.3).

The climate models used in this study are GFDL-ESM4, IPSL-CM6A-LR, MPI-ESM1.2-HR, MRI-ESM2–0, and UKESM1–0-LL. These correspond to the subset selected by the Inter-Sectoral Impact Model Intercomparison Project (ISIMIP), which ensures representation of the full CMIP6 ensemble by including models that differ in structure, process representation, and climate sensitivity (Lange, 2021). Each model contributes distinct strengths: GFDL-ESM4 features high climate sensitivity and a detailed ocean–atmosphere coupling (Dunne et al., 2020); IPSL-CM6A-LR emphasizes land-surface feedbacks and biogeochemical cycles (Boucher et al., 2020); MPI-ESM1.2-HR provides high-resolution representation of extreme events (Gutjahr et al., 2019); MRI-ESM2–0 incorporates improved radiation and cloud interaction (Yukimoto et al., 2019); and UKESM1–0-LL integrates interactive chemistry-climate processes (Sellar et al., 2020).

These models represent distinct representations of the Earth system under the same forcing pathways. The subset was selected to ensure structural independence, model diversity, and robust performance in reproducing historical climate variability, while maintaining data availability across all Shared Socioeconomic Pathways (SSPs) (Eyring et al., 2016a).

Using multiple models instead of a single one or their ensemble mean allows us to better capture structural uncertainty; the variability arising from differences in model formulations, parameterizations, and physical feedbacks. Averaging all models could mask this variability and give a misleading sense of certainty about future projections. By analyzing results across these five models, we capture a realistic range of possible climate futures and can evaluate the robustness of our conclusions across different modeling approaches. This strategy aligns with ISIMIP's multi-model philosophy, which prioritizes the exploration of uncertainty over model optimization or tuning (Dey et al., 2022; Mousavikhaledi et al., 2025).

The selected models were bias-adjusted and statistically downscaled using the ISIMIP3BASD algorithm (Lange, 2021). This method, also applied within ISIMIP, employs a consistent statistical framework that ensure the corrected outputs are applicable at any location worldwide. In line with the ISIMIP protocol, the W5E5 observational dataset (Lange, 2019a) was used as reference for the bias adjustment, which itself is based on ERA5-Land, thereby guaranteeing consistency with local climate conditions. The training period for the downscaling and bias adjustment was 1979–2014. Prior downscaling, the original CMIP6 outputs were harmonized in time and interpolated in space to enable their application with in the ISIMIP3BASD framework (Lange, 2019a).

The resulting database is provided at a spatial resolution of approximately 9 km, corresponding to the W5E5-ERA5-Land grid. While this resolution is coarser than the urban area of Valencia (≈52 km^2), it represents the finest publicly available bias-corrected CMIP6 dataset that consistently covers both the historical (1979–2014) and projected (2015–2100) periods. Similar studies applying regional or downscaled CMIP6 data to urban and peri-urban areas have used comparable spatial resolutions, supporting its suitability for regional-scale heatwave analysis (Chapman et al., 2023; Gilabert et al., 2021; Schwingshackl et al., 2024; Yu et al., 2025).

To address the scale mismatch between the model grid and the city boundaries, spatial interpolation was applied. Although this resolution cannot fully capture local microclimatic variability, it reliably represents regional heatwave trends, which aligns with the scope and objectives of this study.

Future climate conditions were analyzed under three SSPs: SSP126, SSP370 and SSP58. SS126 represents a low-forcing pathway, corresponding to strong mitigation efforts and limited warming by 2100, making it relevant for analyses of achievable climate policy goals. SSP370 represents a medium-to-high forcing pathway, serving as a baseline scenario to quantify the potential impacts of unmitigated emissions and providing insights into social and land use vulnerabilities under intermediate conditions. SSP585 represents a high-forcing pathway, corresponding to the upper bound of projected emissions and warming, and is particularly useful for studying the consequences of extreme scenarios. Together, these three scenarios allow for a comprehensive assessment of heatwave risk under contrasting socioeconomic development trajectories and land use changes (O'Neill et al., 2016; Peano et al., 2022).

In the Valencian Region, heatwave is defined by the Conselleria de Sanitat of the Generalitat Valenciana as a period of at least three consecutive days in which the maximum temperature exceeds the specific threshold temperature of each municipality. This threshold corresponds to the 90th percentile of the maximum daily temperature for the historical period (Laboratorio de Salud Pública y Sanidad Ambiental, 2024).

Heatwaves are characterized by four main aspects:

- Duration: Number of consecutive days with temperatures above the threshold.
- Frequency: Number of events in a period.
- Intensity: Temperature deviation from the threshold, also considering relative humidity.
- Spatial extent: Area affected by the phenomenon.

The analysis integrates duration, frequency, and intensity to provide a detailed diagnosis of heatwaves and their future evolution in the study region.

The threshold temperature used in the analysis corresponds to the 90th percentile of the historical series (1979–2014), determined by month and calculated individually for each model. This threshold is defined in the Program of prevention and attention to health problems derived from high temperatures in the Valencian Region (Laboratorio de Salud Pública y Sanidad Ambiental, 2024).

Several thermal indices were considered in the design of this study, including both empirical indicators (Heat Index (Monteiro et al., 2013; Zuo et al., 2015), Humidex (Katavoutas and Founda, 2019)) and more complex thermal stress indices (Wet Bulb Globe Temperature (WBGT) (Engel et al., 2025), Universal Thermal Climate Index (UTCI) (Katavoutas and Founda, 2019), Physiological Equivalent Temperature (PET)(Díaz-Poso et al., 2023)) (Yin et al., 2022). While indices such as UTCI o Humidex provide a more detailed representation of human thermal stress by incorporating additional variables (radiant temperature, wind speed, or metabolic activity), their computation requires high-resolution input data (Katavoutas and Founda, 2019).

The Heat Index (HI) only requires air temperature and relative humidity, two variables that are robustly provided in climate datasets and particularly relevant for the Mediterranean context. Valencia is characterized by both high summer temperatures and elevated humidity levels, making HI especially suitable to capture perceived heat stress. Moreover, HI has been widely applied in epidemiological and climate health studies due to its simplicity, interpretability, and the direct classification of health risk categories (Monteiro et al., 2013; Zuo et al., 2015).

For these reasons, and after reviewing several alternatives, the Heat Index was selected as the most appropriate indicator for this study, as its feasibility with available data.

The HI allows a direct estimation of the negative health impacts of heatwaves, as it combines air temperature and relative humidity to determine how hot it feels. The following empirical equation, adapted from Awasthi et al. (2022), was used to calculate the heat index. It is important to note that this formula has certain mathematical restrictions: the air temperature must be above 26 °C and the relative humidity must exceed 39 % (Awasthi et al., 2022; Monteiro et al., 2013).

$$HI = -42,379 + 2,049 \bullet T + 10,143 \bullet RH - 0,225 \bullet T \bullet RH - 6,838x10^{-3} \bullet T^2 - 5,448x10^{-2} \bullet RH^2 + 1,229x10^{-3} \bullet T^2 \bullet RH + 8,528x10^{-4} \bullet T \bullet RH^2 - 1,99x10^{-6} \bullet T^2 \bullet RH^2$$

where **T** represents temperature (°F) and **RH** represents relative humidity (%) (Awasthi et al., 2022).

The study area is influenced by four data points, spatial interpolation is needed to obtain a unified time series of maximum temperature and relative humidity. To achieve this, the inverse distance weighted (IDW) interpolation technique was applied. The calculation was performed at the centroid of the study area, weighing the influence of each point according to its proximity to the centroid. The formula used is based on (Daya Sagar et al., 2023).

$$B_i = \frac{1}{(Distance^2)_i}$$

$$A_i = Indicator_i \bullet B_i$$

$$IDW = \frac{\sum A}{\sum B}$$

$$Indicator = T_{max}(^{\circ}C)\ o\ RH(\%)$$

Where the indicator can be either the maximum temperature (**Tmax**) or the relative humidity (**RH**).

With the unified temperature obtained by interpolation, each record was compared with the threshold temperature, which is specifically calculated for each month of analysis. This threshold varies from month to month and is determined based on observed data and model temperatures from the period 1979–2014. A day was classified as a *hot day* when the maximum temperature exceeded the corresponding monthly threshold. When three or more hot days occurred consecutively, the period was classified as a *heatwave event*.

For each identified heatwave event, a set of parameters was calculated:

1. **Start:** Date of the first hot day in the sequence.
2. **End:** Date of the last consecutive hot day.
3. **Duration of event:** Total number of consecutive days on which maximum temperatures exceed the critical threshold.
4. **Maximum temperature of the event:** Highest temperature recorded during the event.
5. **Sum of the thermal anomalies:** Sum of the differences between the daily temperatures and the threshold temperature during the entire event, providing a measure of the overall intensity.
6. **Sum of heat index anomalies:** The heat index (HI) of each hot day was compared with a critical reference value of 32 °C, which marks the threshold at which health problems such as heatstroke, muscle cramps or heat exhaustion can occur. As such, this indicator is the sum of the differences between the heat index and 32 °C over the entire event, providing a measure of cumulative intensity.

This methodology allows us to assess not only the occurrence and characteristics of heatwaves, but also their potential impact on human health by integrating the analysis of the heat index on extreme days.

3.1.2. Trend analysis

To evaluate how heatwaves have changed and could change in terms of frequency, intensity and duration over time, several variables were defined. The frequency of events was quantified as the total number of heatwaves per year, allowing us to identify gradual or more accelerated increase in future scenarios. Total intensity was calculated as the sum of the heat anomalies (difference between maximum and threshold temperature) of all heatwave events in a year, providing an indication that heatwaves are not only more frequent, but that their cumulative impact is greater, reflecting an increase in heat stress. Maximum intensity corresponds to the highest thermal anomaly recorded during any event in the year, highlighting the occurrence of extreme temperature peaks. Similarly, total duration or accumulated number of days was measured as the sum of the duration of all heatwave events in a year, revealing whether heatwaves events are not only more frequent but are also lasting more days in total per year, while maximum duration captures the longest single heatwave, suggesting the increasing prevalence of prolonged events.

For each variable, line graphs were constructed with years (1979–2100) on the X-axis and the annual values of the analyzed variables on Y-axis. Years were divided into four key periods: historical (1979–2014); short term (2015–2044); medium term (2045–2074) and long term (2075–2100). Trend lines for each period were estimated using linear regression, obtaining the gradient, which indicates the annual rate of change of each variable.

In addition, we employed multidimensional visualizations to explore the relationships between heatwave characteristics. Bubble diagram was constructed to relate the duration of heatwaves to their intensity and accumulated impact, and to be able to observe hazard and exposure. In these diagrams, the X-axis represents consecutive days in heatwaves; the Y-axis show the maximum heat index reached during the event; the bubble size indicates the cumulative sum of heat index anomalies, and color denotes the year of occurrence. This representation allows simultaneous visualization of intensity, duration, and temporal distribution of heatwaves, illustrating their progression over time (Fig. 3 & Fig. 4).

Finally, heat map of the maximum temperature during heatwaves by month was elaborated to visualize the monthly evolution of extreme temperatures during heatwaves. For each month, the minimum, mean and maximum of the maximum temperatures recorded during heatwaves were calculated, and the resulting values were represented using a color scale, with months on the X-axis and years or periods on the Y-axis. This approach highlights both temporal and seasonal patterns of temperature extremes, facilitating the identification of months with higher risk of intense heatwaves (Fig. 5).

4. Results

4.1. Observations for the reference period

This study evaluated how heatwaves have changed in terms of frequency, intensity, and duration from 1979 to 2014. To quantify these changes, several variables were analyzed: the total number of heatwave events per year, the total increase in intensity (sum of the thermal anomalies of all events in a year), the maximum intensity recorded in a single event, the total duration of heatwave days per year, and the maximum duration of an individual event. A time series analysis was conducted by plotting the annual values of each

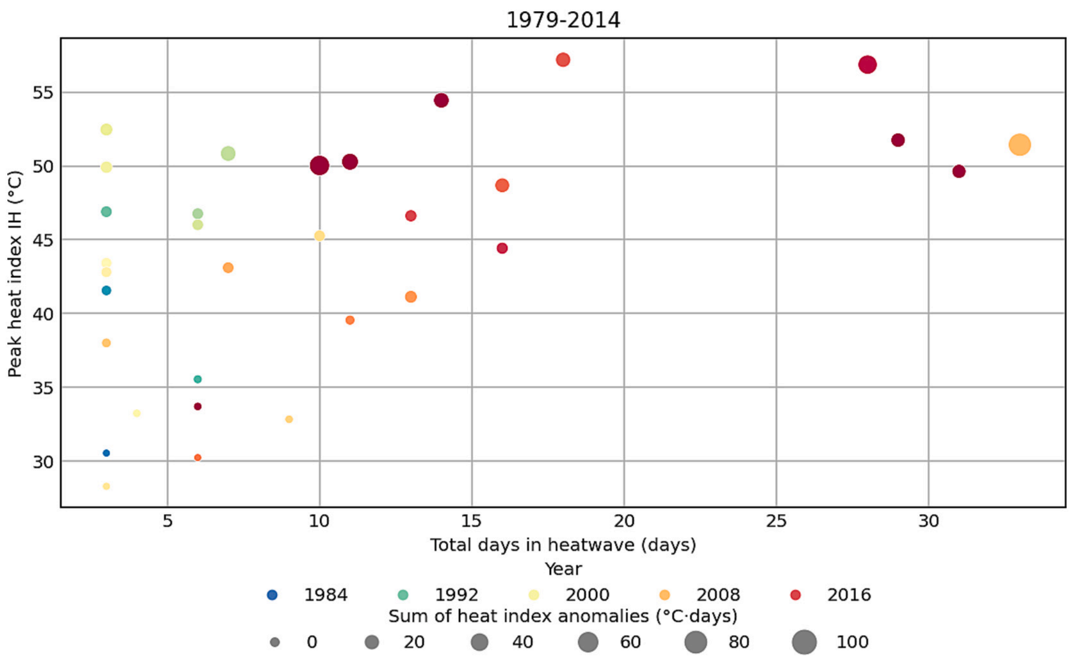

Fig. 3. Hazard and exposure to heatwave events 1979–2014 (W5E5-ERA5-Land).

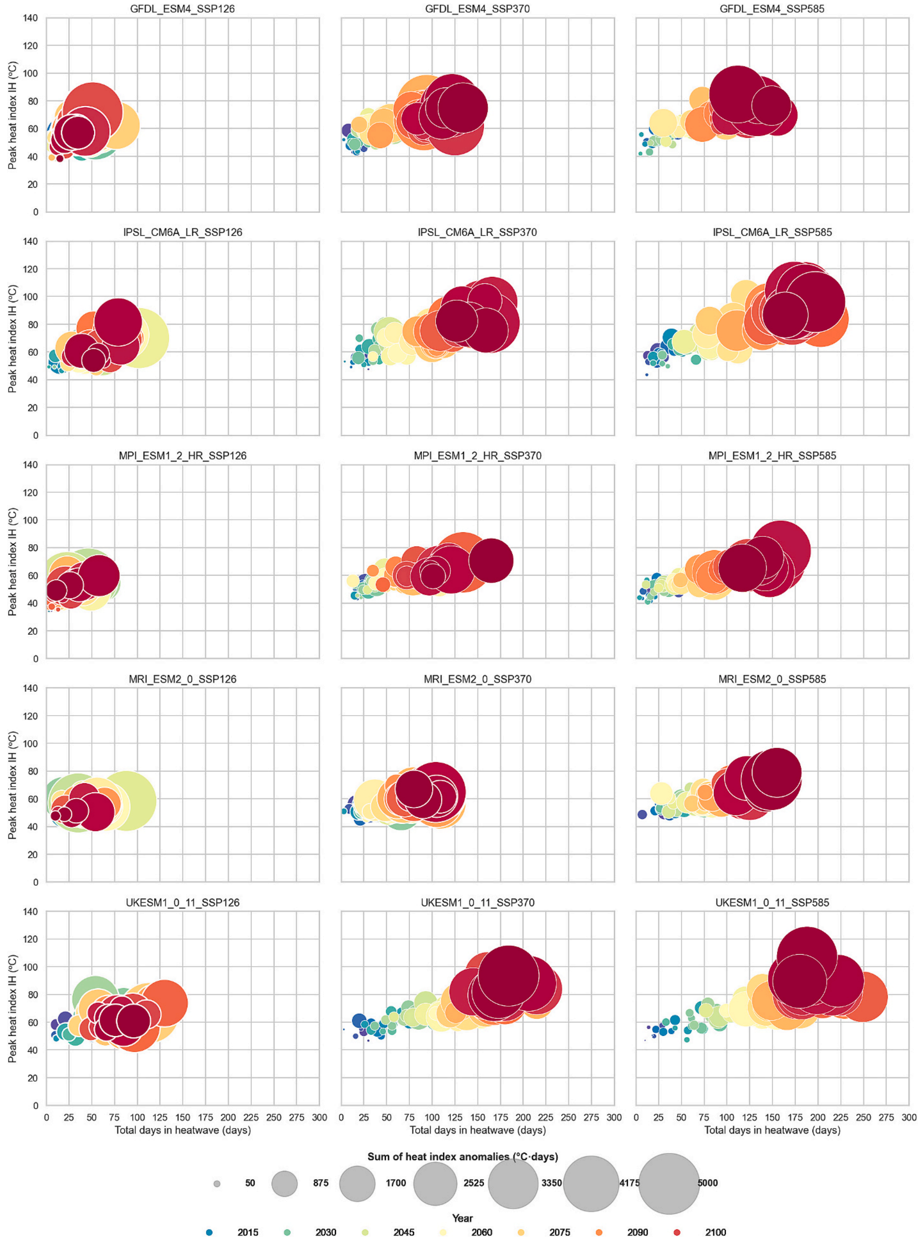

Fig. 4. Hazard and exposure to heatwave events (2015–2100).

variable on the Y-axis against the years on the X-axis. A linear regression was applied to obtain the slope of the trend line, which represents the annual rate of change for each variable. Table 1 summarizes these slopes, indicating how each characteristic of heatwaves has evolved over time.

The historical analysis shows a progressive increase in heatwave frequency, duration, and intensity (Table 1). The number of heatwave events increased rate of 1.87 events per decade in the reference dataset (W5E5-ERA5-Land). With values ranging between 0.62 and 2.10 events per decade across the climate models. The maximum intensity of individual events increased by 2.44 °C per decade on average, reaching values of up to 3.77 °C per decade in the UKESM1–011 model. Event duration also increased, with historical trends of 0.91 days per decade for total duration and 0.58 days per decade for maximum duration.

The differences observed between the models arise from their distinct physical representations and algorithmic emphases. For example, models such as UKESM1–0-LL, which include more detailed radiation, aerosol, cloud interactions and higher climate sensitivity, tend to simulate stronger warming and more intense heatwaves. In contrast, models like MPI-ESM1.2-HR prioritize high spatial resolution and dynamic processes, leading to different patterns in the frequency and duration of events. These structural and parametric differences explain the variability observed in heatwave trends across models.

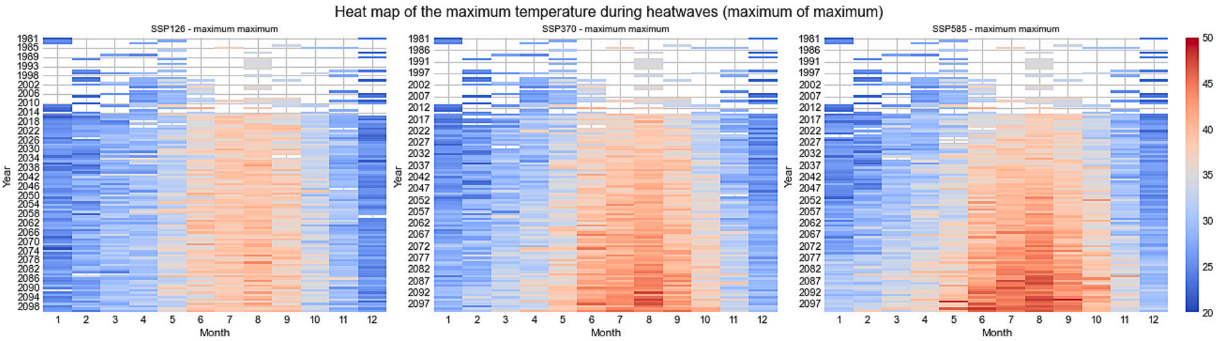

Fig. 5. Heat map of the maximum of maximum temperature during heatwaves by month.

Table 1
Historical evolution of heatwaves in the study area of the Valencia Region (1979–2014).

Period	Annual increase in number of events (event/decade)	Annual increase in intensity (°C/decade)		Annual Increase in duration (days/decade)	
		Total	Maximum	Total	Maximum
W5E5-ERA5-Land	**1.87**	**3.68**	**0.91**	**7.05**	**0.58**
GFDL_ESM4	0.83	1.75	−0.12	4.19	0.57
IPSL_CM6A_LR	1.15	1.60	0.52	4.03	0.10
MPI_ESM1_2_HR	0.62	1.74	0.44	2.39	0.07
MRI_ESM2_0	1.26	3.35	0.69	5.56	0.68
UKESM1_0_11	2.10	3.77	0.54	10.06	1.52
Minimum	**0.62**	**1.60**	**−0.12**	**2.39**	**0.07**
Average	**1.19**	**2.44**	**0.41**	**5.24**	**0.59**
Maximum	**2.10**	**3.77**	**0.69**	**10.06**	**1.52**

To analyze the exposure and severity of these events, a bubble chart was created in Fig. *3*. This multidimensional representation illustrates the combined evolution of event duration, intensity and anomalies. There has been a significant increase in the total duration of these events since 2010. Before 2010, heatwaves typically lasted between 5 and 10 days, whereas after 2010 several events extended beyond 20 days, including 25 days events in 2011, 2012 and 2013. Peak values of the heat index exceeded 50 °C during this period, and the cumulative anomalies greater than 40 °C days were observed after 2004.

4.2. Future projections

The results indicate that the rates of change observed during the period (1979–2014) not only persist but intensify with distinct behaviors depending on the emission pathway, as detailed in Table A. 1.

Table A. 1 shows the predicted evolution of heatwaves in terms of frequency, duration and intensity for the different models and future scenarios (SSP126, SSP370 and SSP585). Fig. *4* complements these results by showing how these trends affect exposure to extreme heat hazard.

Over the period 2015–2044, all scenarios increase of 1–2 events per decade (Table A. 1), consistent with the clustered patterns of points observed in Fig. 4. Between 2045 and 2074, SSP126 shows stabilization, while SSP370 and SSP585 continue to increase, with rates up to 3 events per decade in some models. In 2075–2100, the average trend decreases, with some models projecting up to −4 events per decade (Table A. 1).

The duration of heatwaves shows a differentiated evolution between the scenarios and periods. In 2015–2044, heatwave duration increases by an average of 2 days per decade (Table A. 1). Between 2045 and 2074, SSP126 projects slight decreases (−1 day per decade), while SSP370 and SSP585 show stronger increases, with maximum values of +17 and + 32 days per decade, respectively. For 2075–2100, SSP126 stabilizes, whereas SSP370 and SSP585 continue increasing, with SSP585 reaching up to +61 days per decade. These projections are reflected in Fig. 4, particularly in models such as IPSL-CM6A-LR and UKESM1–0-11, which display strong growth in duration.

In terms of intensity, over the period 2015–2044 the increase in maximum heat index intensity ranges from +5 to +7 °C per decade, with some models reaching +12 °C per decade (Table A. 1). Between 2045 and 2074, intensity continues increasing, with maximum slopes of +12.3 °C per decade in SSP585 continue increasing, reaching values up to +16 °C per decade. These trends are clearly represented in Fig. 4, where the slope of the intensity curves steepens after 2055, especially in SSP585.

The combined results of Table A. 1 and Fig. 4 highlight the progressive intensification of heatwaves throughout the 21st century, with clear trends toward more events, longer duration and more extreme temperatures in the SSP370 and SSP585 scenarios. Although some models in the SSP126 scenario show signs of stabilization or reduction of these effects toward the end of the century, overall, the frequency and intensity of heatwaves will remain above historical values.

To analyze the monthly evolution of extreme temperatures during heatwaves, the seasonal and temporal patterns of these events were identified, highlighting the months with the highest risk of intense heat events in the future, in the heat map (Fig. 5). Historically, heatwaves have been concentrated in the summer, but in the future, they will be more frequent and with higher intensities in other seasons, starting earlier in the year. August will continue to be the warmest month with the highest number of heatwave events in all scenarios. In addition, the distribution of these events is not symmetrical around the warmest month, as the period will extend to spring more than autumn. By the end of the century, periods with extreme temperatures will extend from April to November, with values above 35 °C in these months. Comparing the SSP370 and SSP585 scenarios, it is observed that the increase in extreme temperatures occurs more rapidly in SSP585, reaching critical values 20 years earlier (2072 in SSP585 versus 2092 in SSP370).

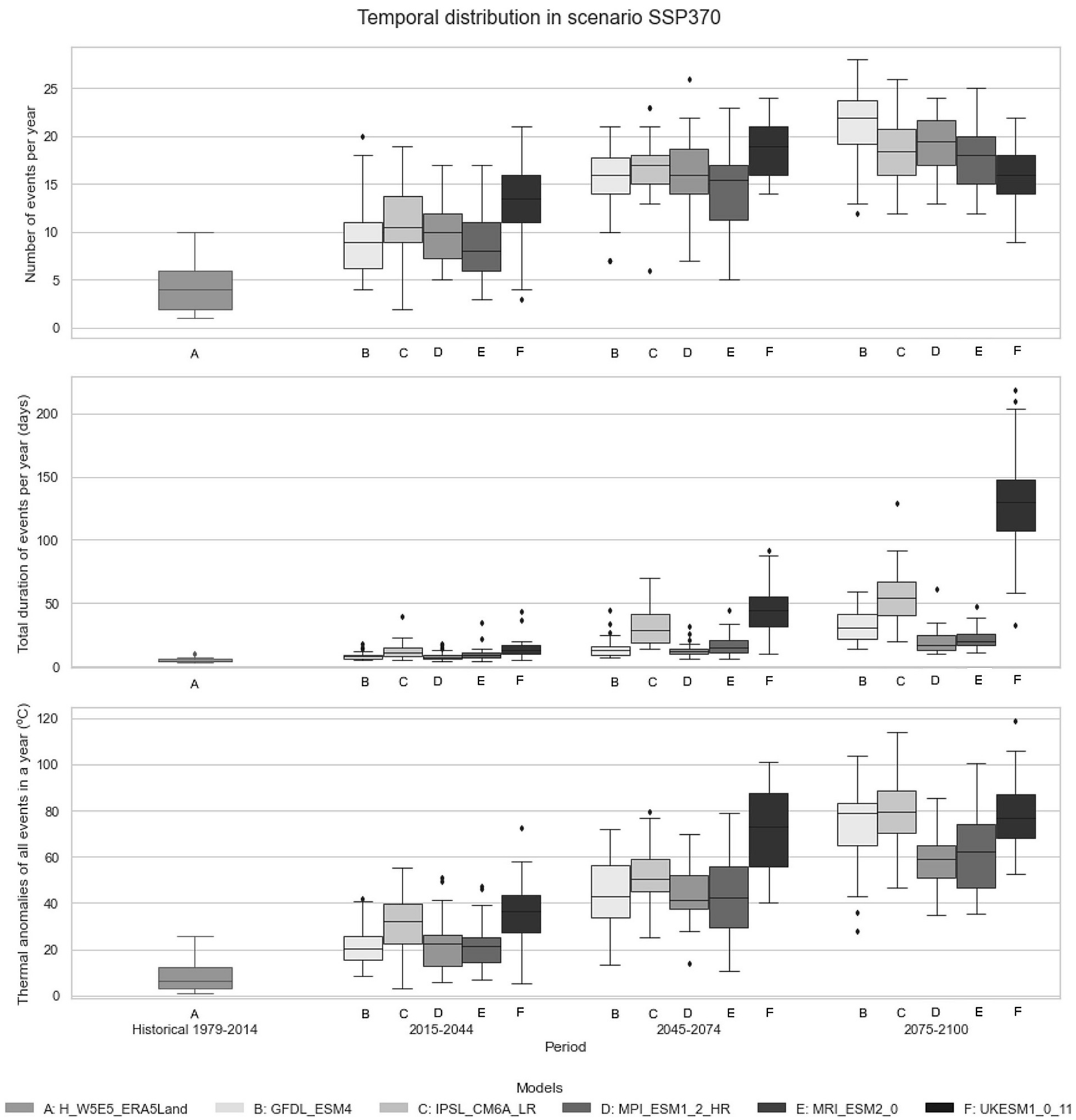

Fig. 6. Temporal distribution in scenario SSP370.

4.3. Uncertainty analysis of heatwave characteristics

Finally, an analysis of the uncertainty in the projections of heatwave characteristics was carried out, considering three key dimensions: the climate models used, the emissions scenarios and the time periods analyzed (1979–2014, 2015–2044, 2045–2074 and 2075–2100). The objective of this analysis was to understand the limitations, variability and structural differences that influence the projections, as well as to identify the factors that generate the greatest uncertainty in the results. The three characteristics assessed were the number of events per year, the duration of heatwaves (days) and the maximum thermal anomaly (°C) recorded during heatwave events. Fig. 6 summarizes the results for the SSP370 scenario; the most likely according to current projections; showing the three variables analyzed. The results for the other two scenarios (SSP126 and SSP585) are available in the Appendix A. Supplementary material to the uncertainty analysis of heatwave characteristics.

In terms of the number of events per year a significant difference is shown between models, scenarios and periods. For example, the UKESM1–0-11 model presents the highest averages in most cases, although in the SSP370 (Fig. 6) and SSP585 (Figure B. 2) scenarios in the period 2075–2100 this decreases significantly. The GFDL-ESM4 model stands out with a high performance in SSP370 and SSP585 during 2075–2100. Inter-model uncertainty clearly increases in high emissions scenarios, especially in the period 2075–2100, where the divergence between medians and the width of the interquartile ranges are more pronounced. At the temporal level, SSP370 (Fig. 6) shows a progressive increase in the number of events, which doubles in 2015–2044, triples in 2045–2074 and reaches a quadrupling in 2075–2100, while SSP585 (Figure B. 2) shows an apparent reduction in 2075–2100, possibly related to the merging of long events. This suggests that the way events are defined and accounted for also influences the interpretation of the projections.

For the duration of heatwaves, uncertainty also increases with the severity of the scenario and the time horizon. Models such as UKESM1–0-11 and IPSL-CM6A-LR tend to project the longest durations, while others such as MPI-ESM1–2-HR and GFDL-ESM4 have better agreement with each other, especially in SSP126 (2045–2074) (Figure B. 1) and SSP370 (Fig. 6) and SSP585 (Figure B. *2*) in the early periods. From 2045 to 2074 onwards, the internal dispersion increases, especially in SSP585, where some models reach mean durations of more than 100 days. UKESM1–0-11 stands out for having larger whiskers and numerous outliers, being the main contributor to the total uncertainty in this variable. These results reflect a high sensitivity of the projections to the choice of model, the emissions scenario and the period analyzed, with UKESM1–0-11 being the clearest example of a model with extreme behavior.

Finally, patterns of uncertainty are also evident in the maximum thermal anomaly. In the first period (2015–2044), the medians are similar between scenarios, but in later periods the differences are amplified. Models such as MPI-ESM1–2-HR and MRI-ESM2–0 tend to project lower anomalies, while UKESM1–0-11 maintains consistently higher ones. The dispersion between models increases especially in 2075–2100, which is reflected in the lengthening of boxes and whiskers. When compared to the historical period, whose median are around 3 °C, all future scenarios show higher values, starting at around 5 °C and increasing progressively. The SSP126 scenario (Figure B. 1) shows a stabilization of the median at the end of the century, while SSP370 (Fig. 6) and SSP585 (Figure B. 2) show a steady increase in both the median and variability, accompanied by a larger number of outliers, particularly in SSP585.

5. Discussion

The objective of this study was to analyze the evolution of maximum temperature and heatwaves in the city of Valencia, focusing on the number of events, their duration, and intensity in the short, medium, and long term. The results show that the intensity and duration of heatwaves have increased since 1979 and that, according to climate models, this rise will continue in the future.

A first relevant finding is that the historical period (1979–2014) already shows a marked warming signal, the intensity of extreme events increased by 3.6 °C, more than double the internationally recognized 1.5 °C critical threshold. This indicates that the Mediterranean region is experiencing a faster warming compared to the Northern Hemisphere average, which is consistent with previous literature identifying the Mediterranean as a climate change hotspot (Masson-Delmotte et al., 2021; Yin et al., 2022). Our historical results (0.91 °C decade and 0.58 days/decade in intensity and duration respectively) are comparable to the global trends reported by Perkins-Kirkpatrick and Lewis (2020), but highlight a stronger amplification in Valencia (Perkins-Kirkpatrick and Lewis, 2020). For example, Australia recorded 0.4–0.6 additional events and heatwaves 2.5 °C hotter per decade between 1911 and 2019 (Jyoteeshkumar Reddy et al., 2021), while in our case the number of events rise to 1.87 and the hottest event increases by 3.86 °C placing the study area at the upper bound of global extremes.

Looking ahead to the future period 2015–2100, our projections indicate increases **frequency** far larger than the global average. While global estimates suggest growth of 0.3 to 0.6 events per decade (Rohini et al., 2019), in Valencia we find up to 3.6 events per decade in SSP 370, an order of magnitude higher. This notable difference could be related to the fact that the Mediterranean will undergo disproportionate impacts, consistent with other regional studies (Perkins-Kirkpatrick and Lewis, 2020; Zacharias et al., 2015).

The projected increase in temperature and heatwave intensity in Valencia is closely linked to the warming of the Mediterranean Sean and associated regional climatic feedbacks. As the sea and surrounding atmosphere become hotter and more humid, conditions will favor more frequent and intense heatwaves. Meanwhile, reduced precipitation and evapotranspiration will lead to vegetation loss and increased exposure of bare soil, enhancing surface heating and local heat stress (Zittis et al., 2022). These land where declining soil moisture and vegetation amplify surface warming, are well documented in Mediterranean regions, showing that regional processes can strongly intensify the effects of global warming on temperature extremes.

As built areas expand, the urban heat island effect will become stronger, trapping heat during the day and releasing it more slowly at night. This means that future heatwaves will likely be accompanied by higher nighttime temperatures, reducing opportunities for thermal recovery and increasing health risks for urban populations (Founda and Santamouris, 2017). Therefore, both climatic and urban factors will play a key role in shaping the future thermal conditions of Valencia.

Intensity also shows unprecedented growth. Perkins-Kirkpatrick and Lewis (2020) estimated increases of 2 to 6 °C per decade in North America, Asia (excluding the Middle East), and Europe. In the city of Valencia, our results are similar for the period 2015–2044, 1.5–12.3 °C depending on scenario, but in later periods the variability is much greater, with maximum projections up to 16 °C per decade in SSP585 for 2075–2100. This represents an intensification several times higher that 0.1–1 °C per decade observed in Germany (Zacharias et al., 2015), evidencing a clear acceleration in Southern Europe.

Duration is another key aspect. For the period 2015–2044, heatwaves are projected to lengthen by 1.7 to 2.3 days per decade across scenarios. These values are consistent with the estimates of Perkins-Kirkpatrick and Lewis (2020), who report increases of 2 to 6.4 days per decade in most regions. However, in the second half of the century the increase become extreme, reaching up to 60.6 days/decade in SSP585. This is drastically higher than the projections for Central and Northern Europe, 0.1–0.4 days/decade (Zacharias et al., 2015). This implies, by the end of the century, heatwaves in Valencia could last for several months, reaching up to 182 days under SSP370 and 319 days under SSP585. These values suggest a radical transformation of the seasonal cycle, we could be facing a permanent "heat season".

While the number of heatwave events increases in the short to medium term, in the period 2075–2100 it tends to decrease. This reduction, however, is not positive: it occurs because events become so prolonged that they overlap, blurring the distinction between separate heatwaves. This phenomenon, rarely emphasized in the literature, suggest that the traditional definition of heatwave (typically three consecutive days above a threshold) may lose relevance in a context where extreme heat can persist for months. We could transition from facing discrete events to living in a quasi-permanent heatwave condition.

This change also affects the timing of events. Historically, heatwaves have been associated with summer, but studies show that they are occurring earlier and extending later in the year (Hulley et al., 2020; Jyoteeshkumar Reddy et al., 2021; Perkins-Kirkpatrick and Lewis, 2020). For instance, in the mid-20th century summer spanned May to August, but now extends from March to September (Hulley et al., 2020). Our analysis supports this expansion: in the study area, extreme temperatures above 35 °C are projected from April to November, extending the "heat season" by more than six months.

Beyond the physical aspects, these findings have serious implications for human health and adaptation. The prolonged duration of heatwaves reduces recovery periods for people, increasing the risk of chronic heat stress, sleep deprivation, and cumulative heath damage. As Hulley et al. (2020) note, adaptation will not only require infrastructure and public health strategies but also a rethinking of how society organizes work, rest, and outdoor activities. Moreover, our analysis, based on the heat index, allows us to quantify not only the thermal conditions but also the potential risk for the population, highlighting that future scenario will lead to increasingly difficult conditions for human well-being (Van Oldenborgh et al., 2022).

Although differences exist among the five CMIP6 models used, these discrepancies reflect the structural and parametric diversity inherent to global climate modeling. Each model incorporates distinct physical representations, that influence projections of heatwave characteristics. The use of multiple models therefore allows us to capture the range of possible futures and quantify the uncertainty of projections. This approach of consider inter-model spread as an essential component of climate risk assessment, ensuring that the conclusions reflect the envelope of credible possibilities for the Mediterranean region.

This study shows that the Mediterranean, and particularly Valencia, is not only following but exceeding global projections of heatwave increase. The observed and projected changes in intensity and duration far surpass those documented in other regions, confirming the area's exceptional vulnerability. The current definitions, metrics, and adaptation strategies may no longer be sufficient.

6. Conclusions

This study has provided insights into the current and future characteristics of heatwaves in the city of Valencia. The results indicate that climate change is not a future phenomenon, but an ongoing reality: since 1979, there has been an increase in the frequency, duration and intensity of heatwaves, and projections indicate that this trend will continue, with longer events and more persistence temperature extremes. These findings highlight the urgent need for adaptation strategies to reduce population vulnerability and mitigate the impacts of climate change in urban environments.

Furthermore, future scenarios suggest a radical transformation of seasonal cycles. Heatwaves may extend from April to November potentially evolving a quasi-permanent "heat season" by the end of the century. Such prolonged events challenge the conventional definition of a heatwave; typically, three consecutive days above a critical threshold, since event lasting several months blur the distinction between discrete episodes. Moreover, the lack of a universally accepted heatwave definition complicates future scenario analyses, as different studies often use varying thresholds, durations, and metrics, which can make difficult to compare results and validate models. As extreme heat became increasingly persistent, current heatwave criteria may become inadequate, necessitating a redefined framework to reflect a future where extreme heat is the norm.

Despite these findings, the results of this study must be interpreted in light of certain limitations inherent to the use of climate models and methodological approaches. Climate models have varying sensitivities to radiative forcing, resulting in uncertainty in future projections; additionally, emissions scenarios (SSP, RCP) are based on assumptions about socioeconomic and technological development, which adds another layer of uncertainty. Moreover, climate models often do not fully capture the localized effects of land use change, urbanization, or deforestation, which may lead to underestimation or overestimation of heatwave impacts in specific regions. In this study, data were interpolated from surrounding grid points to the centroid of the study area, a procedure that may not fully reflect localized thermal variations. Finally, the present analysis does not yet account for the urban heat island effect, which is known to exacerbate heatwave intensity in urbanized zones.

CRediT authorship contribution statement

Ana Fernandez-Garza: Writing – original draft, Visualization, Validation, Software, Methodology, Investigation, Formal analysis, Conceptualization. **Eric Gielen:** Writing – review & editing, Visualization, Supervision, Methodology, Conceptualization. **Manuel Pulido-Velazquez:** Writing – review & editing, Supervision, Funding acquisition, Conceptualization. **Dariana Avila-Velasquez:** Writing – review & editing, Visualization, Data curation, Conceptualization. **Adria Rubio-Martin:** Writing – review & editing, Visualization, Supervision, Software, Project administration, Conceptualization. **Hector Macian-Sorribes:** Writing – review & editing, Visualization, Software, Conceptualization.

Declaration of competing interest

The authors declare the following financial interests/personal relationships which may be considered as potential competing interests:

Ana Fernandez Garza reports financial support was provided by European Union. Dariana Avila-Velasquez reports financial support was provided by Government of Spain Ministry of Universities. If there are other authors, they declare that they have no known competing financial interests or personal relationships that could have appeared to influence the work reported in this paper.

Acknowledgments

This study has received funding from “THE HUT Project” (The Human-Tech Nexus - Building a Safe Haven to cope with Climate Extremes), within the European Union’s Research and Innovation Program (GA No. 101073957).

Bias-adjusted climate change scenarios were developed by CMCC in the context of the European Union’s Horizon 2020 GoNEXUS Project (grant agreement No 101003722).

Dariana Avila-Velasquez acknowledges the financial support received through the University Teacher Training (FPU) contract of the Ministry of Universities (FPU20/0749).

Appendix A. Supplementary data

Supplementary data to this article can be found online at https://doi.org/10.1016/j.uclim.2025.102681.

Data availability

The data that support the findings of this study are available from the corresponding author upon reasonable request.

References

Adger, W.N., 2006. Vulnerability. Glob. Environ. Chang. 16 (3), 268–281. https://doi.org/10.1016/j.gloenvcha.2006.02.006.

Agencia Estatal de Meteorología, 2023. MINISTERIO PARA LA TRANSICIÓN ECOLÓGICA Y EL RETO DEMOGRÁFICO Agencia Estatal de Meteorología Temperatura estimada en la Comunitat Valenciana 10 valores más altos de temperatura máxima, mínima y media 1950-2023 Temperatura MÁXIMA media Temperatura MÍNIMA media Temperatura MEDIA. https://www.aemet.es/documentos/es/serviciosclimaticos/vigilancia_clima/resumenes_climat/ccaa/comunitat-valenciana/avance-climat_val_ago_2023.pdf.

Ajuntament de València, 2025. Actividad económica - Valencia. https://www.valencia.es/cas/la-ciudad/actividad-economica.

Awasthi, A., Vishwakarma, K., Pattnayak, K.C., 2022. Retrospection of heatwave and heat index. Theor. Appl. Climatol. 147 (1–2), 589–604. https://doi.org/10.1007/s00704-021-03854-z.

Boucher, O., Servonnat, J., Albright, A.L., Aumont, O., Balkanski, Y., Bastrikov, V., Bekki, S., Bonnet, R., Bony, S., Bopp, L., Braconnot, P., Brockmann, P., Cadule, P., Caubel, A., Cheruy, F., Codron, F., Cozic, A., Cugnet, D., D’Andrea, F., Vuichard, N., 2020. Presentation and evaluation of the IPSL-CM6A-LR climate model. J. Adv. Model. Earth Syst. 12 (7). https://doi.org/10.1029/2019MS002010.

Cedar Lake Ventures, I, 2025. Weather Spark. https://es.weatherspark.com/y/42614/Clima-promedio-en-Valencia-Espa%C3%B1a-durante-todo-el-a%C3%B1o.

Chapman, S., Syktus, J., Trancoso, R., Thatcher, M., Toombs, N., Wong, K.K.H., Takbash, A., 2023. Evaluation of dynamically downscaled CMIP6-CCAM models over Australia. Earth’s Future 11 (11). https://doi.org/10.1029/2023EF003548.

Cos, J., Doblas-Reyes, F., Jury, M., Marcos, R., Bretonnière, P.A., Samsó, M., 2022. The Mediterranean climate change hotspot in the CMIP5 and CMIP6 projections. Earth Syst. Dynam. 13 (1), 321–340. https://doi.org/10.5194/esd-13-321-2022.

Daya Sagar, Cheng, Q., Mckinley, J., Agterberg, F., 2023. Encyclopedia of Earth Sciences Series Encyclopedia of Mathematical Geosciences.

Dey, A., Sahoo, D.P., Kumar, R., Remesan, R., 2022. A multimodel ensemble machine learning approach for CMIP6 climate model projections in an Indian River basin. Int. J. Climatol. 42 (16), 9215–9236. https://doi.org/10.1002/joc.7813.

Díaz, J., Sáez, M., Carmona, R., Mirón, I.J., Barceló, M.A., Luna, M.Y., Linares, C., 2019. Mortality attributable to high temperatures over the 2021–2050 and 2051–2100 time horizons in Spain: adaptation and economic estimate. Environ. Res. 172, 475–485. https://doi.org/10.1016/j.envres.2019.02.041.

Díaz-Poso, A., Lorenzo, N., Royé, D., 2023. Spatio-temporal evolution of heat waves severity and expansion across the Iberian Peninsula and Balearic islands. Environ. Res. 217. https://doi.org/10.1016/j.envres.2022.114864.

Dunne, J.P., Horowitz, L.W., Adcroft, A.J., Ginoux, P., Held, I.M., John, J.G., Krasting, J.P., Malyshev, S., Naik, V., Paulot, F., Shevliakova, E., Stock, C.A., Zadeh, N., Balaji, V., Blanton, C., Dunne, K.A., Dupuis, C., Durachta, J., Dussin, R., Zhao, M., 2020. The GFDL earth system model version 4.1 (GFDL-ESM 4.1): overall coupled model description and simulation characteristics. J. Adv. Model. Earth Syst. 12 (11). https://doi.org/10.1029/2019MS002015.

Engel, R., Mackres, E., Palmieri, M., Anzilotti, E., 2025, March 17. Beyond the Thermometer: 5 Heat Metrics that Drive Better Decision-Making. https://www.wri.org/insights/beyond-thermometer-measuring-heat.

Eyring, V., Bony, S., Meehl, G.A., Senior, C.A., Stevens, B., Stouffer, R.J., Taylor, K.E., 2016a. Overview of the coupled model intercomparison project phase 6 (CMIP6) experimental design and organization. Geosci. Model Dev. 9 (5), 1937–1958. https://doi.org/10.5194/gmd-9-1937-2016.

Eyring, V., Gleckler, P.J., Heinze, C., Stouffer, R.J., Taylor, K.E., Balaji, V., Guilyardi, E., Joussaume, S., Kindermann, S., Lawrence, B.N., Meehl, G.A., Righi, M., Williams, D.N., 2016b. Towards improved and more routine Earth system model evaluation in CMIP. Earth Syst. Dynam. 7 (4), 813–830. https://doi.org/10.5194/esd-7-813-2016.

Falchetta, G., De Cian, E., Sue Wing, I., Carr, D., 2024. Global projections of heat exposure of older adults. Nat. Commun. 15 (1). https://doi.org/10.1038/s41467-024-47197-5.

Founda, D., Santamouris, M., 2017. Synergies between urban Heat Island and heat waves in Athens (Greece), during an extremely hot summer (2012). Sci. Rep. 7. https://doi.org/10.1038/s41598-017-11407-6.

Gilabert, J., Ventura, S., Segura, R., Martilli, A., Badia, A., Llasat, C., Corbera, J., Villalba, G., 2021. Abating heat waves in a coastal Mediterranean city: What can cool roofs and vegetation contribute? Urban Clim. 37. https://doi.org/10.1016/j.uclim.2021.100863.

Gutjahr, O., Putrasahan, D., Lohmann, K., Jungclaus, J.H., Von Storch, J.S., Brüggemann, N., Haak, H., Stössel, A., 2019. Max Planck institute earth system model (MPI-ESM1.2) for the high-resolution model intercomparison project (HighResMIP). Geosci. Model Dev. 12 (7), 3241–3281. https://doi.org/10.5194/gmd-12-3241-2019.

Hari, V., Rakovec, O., Markonis, Y., Hanel, M., Kumar, R., 2020. Increased future occurrences of the exceptional 2018–2019 central European drought under global warming. Sci. Rep. 10 (1). https://doi.org/10.1038/s41598-020-68872-9.

Hirsch, A.L., Ridder, N.N., Perkins-Kirkpatrick, S.E., Ukkola, A., 2021. CMIP6 MultiModel evaluation of present-day heatwave attributes. Geophys. Res. Lett. 48 (22). https://doi.org/10.1029/2021GL095161.

Hulley, G.C., Dousset, B., Kahn, B.H., 2020. Rising trends in heatwave metrics across Southern California. Earth's Future 8 (7). https://doi.org/10.1029/2020EF001480.

Instituto Nacional de Estadística, 2024. Población por municipios, sexo y edad (año a año). https://www.ine.es/jaxi/Tabla.htm?path=/t20/e244/avance/p02/l0/&file=1mun46.px&L=0.

Intergovernmental Panel on Climate Change (IPCC), 2023. Weather and climate extreme events in a changing climate. In: Climate Change 2021 – The Physical Science Basis. Cambridge University Press, pp. 1513–1766. https://doi.org/10.1017/9781009157896.013.

Jyoteeshkumar Reddy, P., Perkins-Kirkpatrick, S.E., Sharples, J.J., 2021. Intensifying Australian heatwave trends and their sensitivity to observational data. Earth's Future 9 (4). https://doi.org/10.1029/2020EF001924.

Katavoutas, G., Founda, D., 2019. Response of urban heat stress to heatwaves in Athens (1960-2017). Atmosphere 10 (9). https://doi.org/10.3390/atmos10090483.

Klingelhöfer, D., Braun, M., Brüggmann, D., Groneberg, D.A., 2023. Heatwaves: does global research reflect the growing threat in the light of climate change? Glob. Health 19 (1). https://doi.org/10.1186/s12992-023-00955-4.

Laboratorio de Salud Pública y Sanidad Ambiental, 2024. Programa De Prevención Y Atención A Los Subdirección General De Seguridad Alimentaria, Laboratorios De Salud Pública Y Sanidad Ambiental.

Lange, S., 2019a. Trend-preserving bias adjustment and statistical downscaling with ISIMIP3BASD (v1.0). Geosci. Model Dev. 12 (7), 3055–3070. https://doi.org/10.5194/gmd-12-3055-2019.

Lange, S., 2019b. WFDE5 over Land Merged with ERA5 over the Ocean (W5E5). https://doi.org/10.5880/pik.2019.023.

Lange, S., 2021. ISIMIP3b bias Adjustment Fact Sheet.

Lhotka, O., Kyselý, J., Farda, A., 2018. Climate change scenarios of heat waves in Central Europe and their uncertainties. Theor. Appl. Climatol. 131 (3–4), 1043–1054. https://doi.org/10.1007/s00704-016-2031-3.

Masson-Delmotte, V., Zhai, P., Chen, Y., Goldfarb, L., Gomis, M.I., Matthews, J.B.R., Berger, S., Huang, M., Yelekçi, O., Yu, R., Zhou, B., Lonnoy, E., Maycock, T.K., Waterfield, T., Leitzell, K., Caud, N., 2021. The Physical Science Basis Summary for Policymakers Technical Summary Frequently Asked Questions Glossary Part of the Working Group I Contribution to the Sixth Assessment Report of the Intergovernmental Panel on Climate Change Edited by. www.ipcc.ch.

Min, S., Merwin Monteiro, J., 2025. Exceptional Climate Conditions in 2023. www.nature.com/collections/ahbedcfifa.

Monteiro, A., Carvalho, V., Velho, S., Sousa, C., 2013. The accuracy of the heat index to explain the excess of mortality and morbidity during heat waves - a case study in a mediterranean climate. Bull. Geograph. 20, 71–84. https://doi.org/10.2478/bog-2013-0012.

Mousavikhaledi, O., Firoozzare, A., Boccia, F., Dourandish, A., Chamanehfar, S., Covino, D., 2025. Multi-model ensemble CMIP6 for prediction of climate changes: evidence from Asia. Environ. Dev. Sustain. https://doi.org/10.1007/s10668-025-06371-5.

O'Neill, B.C., Tebaldi, C., Van Vuuren, D.P., Eyring, V., Friedlingstein, P., Hurtt, G., Knutti, R., Kriegler, E., Lamarque, J.F., Lowe, J., Meehl, G.A., Moss, R., Riahi, K., Sanderson, B.M., 2016. The scenario model intercomparison project (ScenarioMIP) for CMIP6. Geosci. Model Dev. 9 (9), 3461–3482. https://doi.org/10.5194/gmd-9-3461-2016.

Ouzeau, G., Soubeyroux, J.M., Schneider, M., Vautard, R., Planton, S., 2016. Heat waves analysis over France in present and future climate: application of a new method on the EURO-CORDEX ensemble. Clim. Serv. 4, 1–12. https://doi.org/10.1016/j.cliser.2016.09.002.

Peano, D., Van Beek, R., Bisselink, B., Macian-Sorribes, H., 2022. D2.1: Global and Continental Climate and Land Use Scenarios Lead by CMCC.

Perkins-Kirkpatrick, S.E., Lewis, S.C., 2020. Increasing trends in regional heatwaves. Nat. Commun. 11 (1). https://doi.org/10.1038/s41467-020-16970-7.

Porja, T., Dhimitri, J., 2019. Heat Waves in Albania, the Estimation of Thom's Thermal Discomfort Index (di), its Geographical Distribution, During Summer, p. 2019.

Robinson, P.J., 2000. On the Definition of a Heat Wave.

Rohini, P., Rajeevan, M., Mukhopadhay, P., 2019. Future projections of heat waves over India from CMIP5 models. Clim. Dyn. 53 (1–2), 975–988. https://doi.org/10.1007/s00382-019-04700-9.

Royé, D., Codesido, R., Tobías, A., Taracido, M., 2020. Heat wave intensity and daily mortality in four of the largest cities of Spain. Environ. Res. 182. https://doi.org/10.1016/j.envres.2019.109027.

Schwingshackl, C., Daloz, A.S., Iles, C., Aunan, K., Sillmann, J., 2024. High-resolution projections of ambient heat for major European cities using different heat metrics. Nat. Hazards Earth Syst. Sci. 24 (1), 331–354. https://doi.org/10.5194/nhess-24-331-2024.

Sellar, A.A., Walton, J., Jones, C.G., Wood, R., Abraham, N.L., Andrejczuk, M., Andrews, M.B., Andrews, T., Archibald, A.T., de Mora, L., Dyson, H., Elkington, M., Ellis, R., Florek, P., Good, P., Gohar, L., Haddad, S., Hardiman, S.C., Hogan, E., Griffiths, P.T., 2020. Implementation of U.K. Earth System Models for CMIP6. J. Adv. Model. Earth Syst. 12 (4). https://doi.org/10.1029/2019MS001946.

Sun, P., Zou, Y., Yao, R., Ma, Z., Bian, Y., Ge, C., Lv, Y., 2023. Compound and successive events of extreme precipitation and extreme runoff under heatwaves based on CMIP6 models. Sci. Total Environ. 878. https://doi.org/10.1016/j.scitotenv.2023.162980.

Van Oldenborgh, G.J., Wehner, M.F., Vautard, R., Otto, F.E.L., Seneviratne, S.I., Stott, P.A., Hegerl, G.C., Philip, S.Y., Kew, S.F., 2022. Attributing and projecting heatwaves is hard: We can do better. In: Earth's Future, vol. 10, Issue 6. John Wiley and Sons Inc. https://doi.org/10.1029/2021EF002271

Wei, L., Sobrino, J.A., 2024. Surface urban heat island analysis based on local climate zones using ECOSTRESS and Landsat data: a case study of Valencia city (Spain). Int. J. Appl. Earth Obs. Geoinf. 130. https://doi.org/10.1016/j.jag.2024.103875.

Yin, C., Yang, Y., Chen, X., Yue, X., Liu, Y., Xin, Y., 2022. Changes in global heat waves and its socioeconomic exposure in a warmer future. Clim. Risk Manag. 38. https://doi.org/10.1016/j.crm.2022.100459.

Yu, J., Moise, A.F., Sahany, S., Prasanna, V., Chua, X.R., Chen, C., Hassim, M.E.E., Lim, G., Luo, F., Kumar, A., Liu, P., Raavi, P.H., 2025. High-resolution dynamically downscaled projections of future extreme temperatures, heatwaves and exposure in Southeast Asia. Sci. Total Environ. 980. https://doi.org/10.1016/j.scitotenv.2025.179501.

Yukimoto, S., Kawai, H., Koshiro, T., Oshima, N., Yoshida, K., Urakawa, S., Tsujino, H., Deushi, M., Tanaka, T., Hosaka, M., Yabu, S., Yoshimura, H., Shindo, E., Mizuta, R., Obata, A., Adachi, Y., Ishii, M., 2019. The meteorological research institute Earth system model version 2.0, MRI-ESM2.0: description and basic evaluation of the physical component. J. Meteorol. Soc. Jpn. 97 (5), 931–965. https://doi.org/10.2151/jmsj.2019-051.

Zacharias, S., Koppe, C., Mücke, H.G., 2015. Climate change effects on heat waves and future heat wave-associated IHD mortality in Germany. Climate 3 (1), 100–117. https://doi.org/10.3390/cli3010100.
Zittis, G., Almazroui, M., Alpert, P., Ciais, P., Cramer, W., Dahdal, Y., Fnais, M., Francis, D., Hadjinicolaou, P., Howari, F., 2022. Climate change and weather extremes in the eastern Mediterranean and Middle East to cite this version. Weather extremes in the eastern Mediterranean and Middle East. Rev. Geophys. 2022 (3). https://doi.org/10.1029/2021rg000762ï, 2021–000762.
Zuo, J., Pullen, S., Palmer, J., Bennetts, H., Chileshe, N., Ma, T., 2015. Impacts of heat waves and corresponding measures: a review. In: Journal of Cleaner Production, vol. 92. Elsevier Ltd., pp. 1–12. https://doi.org/10.1016/j.jclepro.2014.12.078